Industrial Health 2015, **53**, 245–259

Original Article

Effect of higher frequency components and duration of vibration on bone tissue alterations in the rat-tail model

Srikara V. PEELUKHANA[1a], Shilpi GOENKA[1a], Brian KIM[1], Jay KIM[1], Amit BHATTACHARYA[2], Keith F. STRINGER[3] and Rupak K. BANERJEE[1]*

[1]Department of Mechanical and Materials Engineering, University of Cincinnati, USA
[2]Department of Environmental Health, University of Cincinnati, USA
[3]Department of Pathology, Cincinnati Children's Hospital Medical Centre, USA

Received May 25, 2014 and accepted January 29, 2015
Published online in J-STAGE April 4, 2015

Abstract: To formulate more accurate guidelines for musculoskeletal disorders (MSD) linked to Hand-Arm Vibration Syndrome (HAVS), delineation of the response of bone tissue under different frequencies and duration of vibration needs elucidation. Rat-tails were vibrated at 125 Hz (9 rats) and 250 Hz (9 rats), at 49 m/s^2, for 1D (6 rats), 5D (6 rats) and 20D (6 rats); D=days (4 h/d). Rats in the control group (6 rats for the vibration groups; 2 each for 1D, 5D, and 20D) were left in their cages, without being subjected to any vibration. Structural and biochemical damages were quantified using empty lacunae count and nitrotyrosine signal-intensity, respectively. One-way repeated-measure mixed-model ANOVA at $p<0.05$ level of significance was used for analysis. In the cortical bone, structural damage quantified through empty lacunae count was significant ($p<0.05$) at 250 Hz (10.82 ± 0.66) in comparison to the control group (7.41 ± 0.76). The biochemical damage was significant ($p<0.05$) at both the 125 Hz and 250 Hz vibration frequencies. The structural damage was significant ($p<0.05$) at 5D for cortical bone while the trabecular bone showed significant ($p<0.05$) damage at 20D time point. Further, the biochemical damage increased with increase in the duration of vibration with a significant ($p<0.05$) damage observed at 20D time point and a near significant change ($p=0.08$) observed at 5D time point. Structural and biochemical changes in bone tissue are dependent upon higher vibration frequencies of 125 Hz, 250 Hz and the duration of vibration (5D, 20D).

Key words: Hand-arm vibration syndrome, Resonance frequency, Osteocyte, Biochemical alterations, Nitrotyrosine

Introduction

Prolonged exposure to hand-transmitted vibrations (HTV) from hand held power tools leads to Hand-Arm Vibration Syndrome (HAVS) which consists of vascular, sensorineural disorders, and musculoskeletal disorders (MSD)[1)]. NIOSH estimates that about half of the 1.2 to 1.5 million US workers who use hand-held powered tools are at risk of developing HAVS[2)]. Various bone disorders such as low bone mineral density, bone lesions and carpal bone abnormalities are caused by vibration[3)]. For example, it has been reported that in the manufacturing sector, workers using hand-held powered tools undergo the

*To whom correspondence should be addressed.
E-mail: Rupak.Banerjee@uc.edu
[a]Both authors contributed equally to the work.

induction of bone lesions and osteonecrosis of the lunate (Kienbocks disease)[4]. In addition, workers in the mining sector develop osteonecrosis of the carpal scaphoid[5]. Some studies have reported that the changes observed after vibration exposure were not different from those found in ageing populations[4]. Elsewhere, it has been reported that vibration altered the bone remodeling and affected bone mineralization[6]. Some studies have reported that low frequency (<40 Hz) vibrations of high magnitude might be associated with abnormal radiological findings in the wrist and elbow joints[4, 7, 8]. Epidemiological data on the quantitative association between vibration and risks of bone degeneration are still inconclusive.

Although there have been a few recent studies on the effects of mechanical vibration on bone[9, 10], the range of vibration frequencies reported in these studies are several orders of magnitude lower than those caused by the pneumatic tools. Pneumatic tool operators in the workplace are exposed to vibration frequencies in the range of 5.6 Hz to 1,400 Hz. Not all frequencies, magnitudes or durations of vibration cause similar effects. These effects are extremely subject specific[3]. It has been reported that the resonance frequency of the human finger tissue is in the range 100–350 Hz[11]. In addition, most of the tools, such as grinders and chipping hammers, used in industrial workplace generate significant vibration components in the *frequency range* 100–400 Hz[12]. However, the current ISO standard 5349-1 and ANSI-standard 2.70 have given greater weight to lower frequencies (<32.5 Hz) and less weight to higher frequencies (>100 Hz)[13]. The validity of this weighting has been questioned by researchers[13–17] who suspect a greater risk of vibration-injury in the case of frequency components higher than the 100 Hz. This ISO guideline, with its higher weightage to lower frequency range, might lead to an under estimation of the risk of high frequency components.

The rat-tail bone (caudal vertebra) has been previously used to study changes in bone tissue morphology and the response of bone under mechanical loading[18–22]. Moreover, the changes induced in bone tissue can be better studied using this model since it has been already validated that the rat-tails' nerves and vasculature surrounding the bone tissue mimic human finger. To the best of our knowledge, this model has not been studied before for the study of vibration-induced bone disruption, in relation to HAVS. Currently, there is a *gap* in the understanding of how higher-frequency components of vibration (>100 Hz) and the duration of vibration induce biological alterations in the bone tissue. Hence, there is a *need* for elucidation of the cellular basis by which bone responds to vibrations, which would aid in identification of novel therapeutic approaches for treatment of musculoskeletal diseases and injuries related to HAVS.

In consideration of the aforementioned factors, in this study we sought to investigate the changes in bone tissue under the influence of vibration at near resonance frequencies and also the duration of vibration, using a rat-tail model of vibration injury. We *hypothesized* that bone tissue alterations, manifested in the form of structural damage (cortical and trabecular bone morphology) and biochemical alterations (nitrotyrosine (NT)-mediated oxidative injury[23, 24] are dependent on the resonance frequencies (125 Hz and 250 Hz) as well as the time duration of vibration exposure. Hence, in the present study, our aim was two-fold: i) quantification of the effects of *vibration frequency* (125 Hz, 250 Hz) on structural and biochemical (oxidative) alterations in bone tissue; and ii) quantification of the effects of *duration of vibration* (1D, 5D, 20D) on structural and biochemical alterations in bone tissue.

Subjects and Methods

Animal Groups. The animal protocol for this study was approved by the Institute for Animal Care and Usage Committee (IACUC) at University of Cincinnati (UC). All procedures were in compliance with the NIH Guide for the Care and Use of Laboratory Animals. Vibration experiments were performed on non-anesthetized male Sprague-Dawley rats (250 ± 15 gm, Harlan Laboratories, WI). The study consisted of a total of 24 rats (Table 1). For the control group, 6 rats were utilized (2 each for 1D, 5D, and 20D). 9 rats were assigned to 125 Hz group (3 rats each for 1D, 5D, and 20D) and 9 rats for the 250 Hz group (3 rats each for 1D, 5D, and 20D). The rats were housed in standard cages in a colony room at 25 ± 1° C with a 12:12 light: dark cycle in the Laboratory for Animal Medicine and Services (LAMS) at UC and were provided the standard rodent diet and tap water.

Vibration Protocol. The vibration experiments were done at frequencies of 125 Hz and 250 Hz, for duration of 4 h/day for 1D, 5D and 20D. The rats were placed in Broome style restrainers resting on a non-vibrating support and the tails were strapped to a platform. In order to avoid any interference to the experimental vibrations, the platform material was selected so that it had a natural frequency higher than 1,000 Hz. Three rats were used at one time for vibration and the tails were symmetrically placed and secured using duct tape (Fig. 1). The rats were

Table 1. The experimental design for the study with the number of animals in each group

Vibration frequency	1D	5D	20D	*Total rats for frequency analysis
Control	n=2	n=2	n=2	6
125 Hz	n=3	n=3	n=3	9
250 Hz	n=3	n=3	n=3	9
*Rats for day analysis	Control = 2, Vibrated = 6	Control = 2, Vibrated = 6	Control = 2, Vibrated = 6	

* number of rats used for the one-way mixed-model data analysis.

monitored during the experiments in order to make sure the tail didn't bounce on/off the platform. This platform was connected to a mechanical shaker (model V203; Ling Dynamic Systems, Herts, UK) which generated vertical vibrations (Fig. 1). Control group rats remained in their respective cages and were not subjected to either the vibration stress or the constraint (straps) stress on the non-vibrating platform. The required sinusoidal frequency was produced by a function generator (Model HP 35660A; HP Inc., Palo Alto, CA, USA) connected to a power amplifier (Model PA 25; Ling Dynamic Systems, Herts, UK). An accelerometer (Model U352B22; PCB group Inc., Buffalo, NY, USA) was attached to the platform to measure and maintain the acceleration at a constant value during the experiment. The acceleration used for both the vibration frequencies was a constant acceleration excitation of 49 m/s^2 RMS. After vibration exposure, rats were returned to their respective cages and housed in the colony room.

Animal Health Observations. The animals were monitored for health and behavior during the time of vibration exposure for all the days of vibration. We did not find any symptoms of chromodacryorrhea (porphyrin secretion) or change in body temperature or teeth grinding, similar to a previously reported study by Yan *et al.*, 2010[25]. Also, the animals did not exhibit any signs of stress or aberrant behavior. Rats in all the groups generally remained calm in the restrainer during the vibration exposure.

Bone Tissue Processing. After vibration exposure, rats were euthanized using carbon dioxide as per standard laboratory procedures followed by a secondary physical method of diaphragm puncture (approved by IACUC at LAMS, UC). The rats were euthanized at similar intervals (within 3 h) from the last vibration exposure. The rat-tail was first fixed in 4% paraformaldehyde for 24 h and one bone sample was harvested from the middle part of the whole tail, from each frequency group. These bone samples were then cleaned of all adhering soft tissues with the help of a sharp scalpel, careful to avoid any damage to the underlying bone. The samples were then stored in a neutral 30% sucrose PBS buffer at 4 °C until they were ready to be prepared for embedding. After dissection, one bone specimen was decalcified in 10% EDTA solution, according to commonly employed histological methodology. Decalcification was checked for completion by chemical testing with ammonium oxalate solution, and it took two weeks for samples to be fully decalcified. Decalcified rat-tail bone was sectioned longitudinally (on a dental wax substrate) and embedded in paraffin.

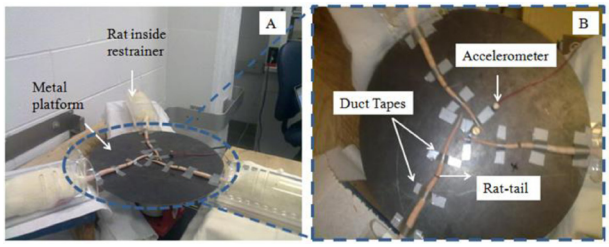

Fig. 1. Experimental set up for the rat-tail vibration.

Further, material characterization tests were performed to augment the data for biochemical changes due to frequency effects at the 20D time point only. In order to achieve this, we harvested a second bone sample from the tails of 20D vibration group rats (Control, 125 Hz, 250 Hz). This bone sample was not decalcified and embedded in acrylic resin (SamplKwik®, Buehler Ltd., Lake Bluff, IL, USA) and prepared for biochemical characterization using material tests of Energy Dispersive X-ray analysis (EDX) and Backscattered Electron microscopy (BSE).

Histological Study for Osteocyte and Empty Lacunae Count. H&E stain was used to stain 4 μm thick sections from paraffin embedded bone blocks on glass slides and subsequently assessed under light microscopy for alterations in the bone structure. After cover-slipping, the slides were assessed at X40 objective magnification for quantification of i) count of viable osteocytes divided by total count of osteocytes and empty lacunae[26] and ii) empty lacunae in five randomly selected fields in the diaphysis of cortical bone using NIH ImageJ program.

Static Histomorphometry. The H&E stained images were used further for assessment of changes in trabecular bone microarchitecture by static histomorphometry. The images were taken at 5× objective magnification and processed in ImageJ. BoneJ plugin[27] was used for calculation of the parameters: trabecular separation (Tb.Sp) and trabecular thickness (Tb.Th). Proximal and distal trabeculae were evaluated from each section for a total of two sections per rat in each group.

Immunohistochemistry. The protocol used for immunohistochemial study is similar to our previous study[28]. Briefly, the paraffin-embedded bone tissues were sectioned at 4 μm, affixed to glass slides and then deparaffinized in xylene and graded series of ethanol, similar to the H&E stained sections. Sections on the slides were rehydrated, washed and blocked with a mixture of 2% goat serum and 2% donkey serum. Subsequently, the sections were incubated with mouse anti-nitrotyrosine primary antibody (Santa Cruz Biotechnology, CA, USA, 1:100, 4 °C) overnight. Following this, the sections were further incubated in biotinylated goat anti-mouse secondary antibody (Ventana, CA, USA, 1:100, 30 min, 25 °C) and developed using peroxidase substrate. Sections were then coverslipped and photographed with a Spot RT Slider digital camera (Diagnostic Instruments, Sterling Heights, MI, USA) mounted on a Nikon Eclipse E600 microscope. An intense brown coloration was indicative of a positive signal. Quantification of NT immuno-staining intensity was done by calculating the GSV (gray scale value) similar to the method we have reported in earlier study[28].

Backscattered Electron Microscopy (BSEM). The resin-embedded bone block was used for Back Scattered Electron Imaging (BSE)-Scanning Electron Microscopy (SEM) using a FEI XL30 ESEM model, equipped with a BSE detector. The bone blocks were coated with a thin layer of Au/Pd to increase the conductivity of the samples and were examined in the electron microscope under the BSE mode. The working distance was 10 mm, working voltage set to 15 kV and the spot size was set to 4. The images were acquired for the cortical bone (diaphysis) for all the groups. A total of 3–5 images were collected in the central part of bone in BSE mode for each rat in each group. The use of BSE images for mineralization distribution has already been demonstrated and there are many studies which have assessed the mineralization distribution curves qualitatively and quantitatively[29–31]. For the assessment of mineralization pattern in the bone, the same BSE images were opened in ImageJ and were cropped and smoothed. The mineralization distribution histogram was then plotted in ImageJ (using Analyze > Histogram command) and the mean grey level values were noted and the mineralization curves were plotted.

Energy Dispersive X-ray Analysis (EDX). Energy Dispersive X-ray Analysis (EDX) was used along with the BSE to further validate the mineralization changes by calculating Ca/P ratio. The Ca/P ratio and its spatial distribution can be a useful predictor of any abnormal alterations occurring in mineralization patterns after vibration of the bone tissue since Ca/P ratio is highly sensitive to changes in bone mineralization. Energy-dispersive X-ray spectroscopy (EDX), coupled with Scanning Electron Microscopy (SEM) in a manner similar to that reported by other researchers[32, 33] was used. Images obtained by SEM (Model: XL-30 ESEM; SN D1398, FEI, Hillsboro, OR, USA) were further used for EDS (EDAX systems (Mahwah, NJ, USA) analysis to obtain Ca (wt%) and the Ca/P ratio at 4–5 randomly sampled points in the diaphysis of central cortical bone sample, per group.

Statistical Analysis. Based on the suggestions from a biostatistician, in order to account for the variability between the multiple sections (repeated measures) and for the variability in data between the rats, a one-way repeated measures mixed-model analysis of variance (ANOVA) was used. The data was checked for normal distribution prior to performing the statistical analysis. A compound symmetry covariance structure was assumed for within the subject (repeated measures) and between the subject (random subject) effects. Please note that the repeated measures involved obtaining multiple data from a single rat at a single time point. It didn't involve a time variation in single rat.

Group mean effects of frequency of vibration on structural damage (osteocyte count) and biochemical damage (NT signal intensity) were assessed. Similarly, the group mean effects of duration of vibration on structural damage (osteocyte count) and biochemical damage (NT signal intensity) were also assessed. In order to assess the interaction effects between the vibration frequency and days of vibration groups, further statistical analysis was performed. This analysis was presented in the Appendix 1.

For osteocyte count quantification, we had 36, 34 and 40 data points from the control (6 rats), 125 Hz (9 rats) and 250 Hz groups (9 rats), respectively (Table 1). For NT signal intensity, we had 13 data points for the control group (6 rats), 23 data points for the 125 Hz group (9 rats) and 18 data points for the 250 Hz group (9 rats) (Table 1). In all the analyses, animal was treated as the random effect while frequency was treated as fixed effect. The number

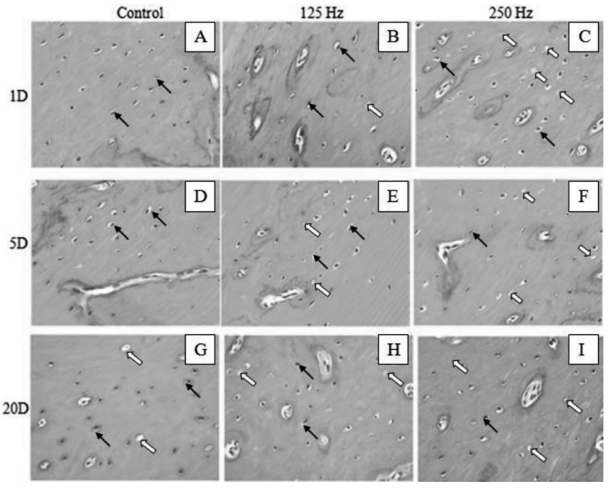

Fig. 2. Photomicrographs of the histological examination of cortical bone in the control and vibrated bone sections using H&E stain. A) Control for 1D; B) 125 Hz for 1D; C) 250 Hz for 1D; D) Control for 5D; E)125 Hz for 5D; F) 250 Hz for 5D; G) Control for 20D; H) 125 Hz for 20D; I) 250 Hz for 20D. Osteocytes are represented by black arrows and the white arrows show empty lacunae in the cortical bone. Magnification is ×40 objective.

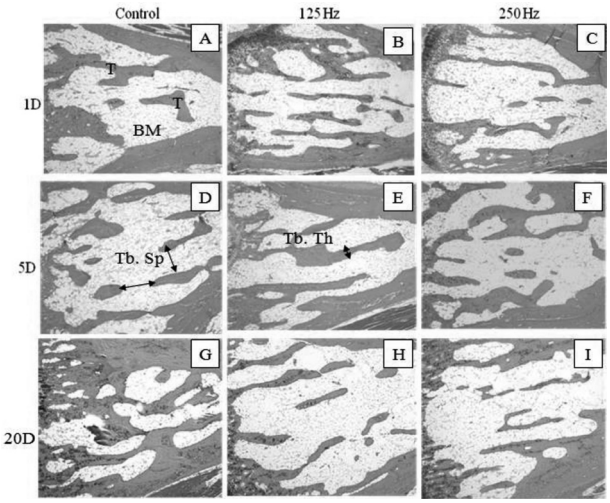

Fig. 3. H&E stained images of trabecular bone in the control and vibrated bone sections.
A) Control for 1D; B) 125 Hz for 1D; C) 250 Hz for 1D; D) Control for 5D; E) 125 Hz for 5D; F) 250 Hz for 5D; G) Control for 20D; H) 125 Hz for 20D; I) 250 Hz for 20D. T represents trabecular bone and BM represents the bone marrow. Magnification is ×5 objective.

of rats (subjects) is the n-value and each data point is considered an observation from each rat. Data analysis was performed using SAS 9.1.3 (SAS Institute Inc., NC, USA) with $p<0.05$ used as the probability level to accept statistical significance. The comparisons were performed using pdiff command. Tukey-kramer and bonferroni adjustments yielded similar *p*-values. All values are reported as mean ± SE.

Power analysis. From Diggle *et al*., 2002[34], number of subjects required to compare means across two groups with repeated measures is given by

$$N = \frac{2(z\alpha + z\beta)^2(1+(n-1)\rho)}{n[(\mu_1 - \mu_2)/\sigma]^2}$$

where, σ=31.67 (obtained from SAS), this is the common variance in the two groups, the $\mu_1-\mu_2$=174.09–168.1=5.97 (obtained from SAS), the difference in means of the two groups. The n=1, this is the number of repeated measures, in this case number of sections from each rat. The lowest number of sections obtained from a rat were used. The ρ=3.75 (obtained from SAS), this is the correlation of the repeated measures. The N is the number of rats per group, 2 was used since that is the least number of rats in the group. Please note that in the above formula, for each of the parameters minimum values were used to provide a conservative estimate. Substituting the values and solving for Z_β=(−1.46), we get the value of β as 0.072. Therefore, the power of the test would be (1−β) × 100, which is 92.8%. This is the least expected power of our comparisons.

Results

The qualitative and quantitative effects of various levels of vibration frequency in bone tissue were assessed by analyzing the structural damage (H&E stained sections for osteocyte and empty lacunae count in cortical bone and trabecular bone micro architecture) and the biochemical damage (NT immunoreactivity obtained by immunohistochemistry). In order to avoid repetition, first the qualitative effects of the vibration frequency and days of vibration are presented briefly. This is followed by an explanation of the quantitative effects of varying vibration frequencies. Subsequently, the quantitative effects of number of days of vibration is discussed.

Qualitative effects of vibration frequency and days of vibration

H&E staining. The results obtained from H&E staining on control and vibrated bone sections are shown in Fig. 2. Qualitative observation shows that 250 Hz causes higher number of empty lacunae as compared to either control or 125 Hz groups. Similarly, when observed across the

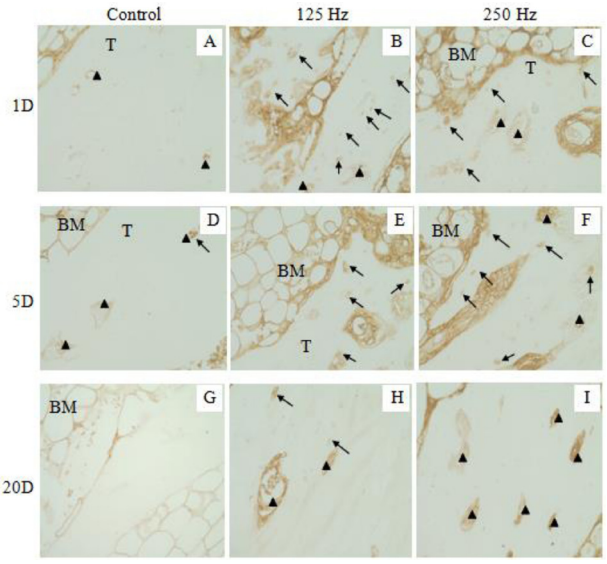

Fig. 4. Representative photomicrographs for NT stained sections for: A) Control for 1D; B) 125 Hz for 1D; C) 250 Hz for 1D; D) Control for 5D; E)125 Hz for 5D; F) 250 Hz for 5D; G) Control for 20D; H) 125 Hz for 20D; I) 250 Hz for 20D. Positive signal in the osteocytes is represented by black arrows and the black triangles show blood vessels in the trabecular bone. Magnification is ×40 objective.

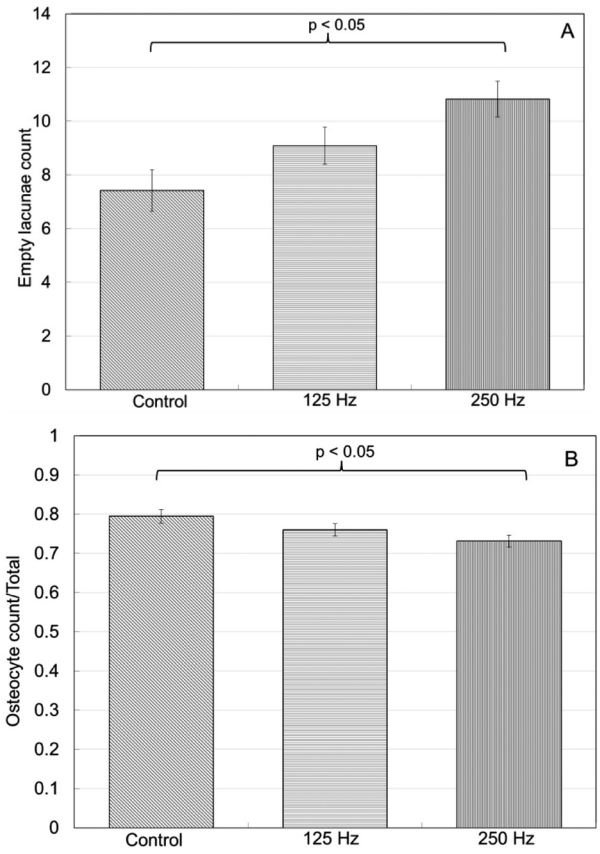

Fig. 5. Bar plots showing the effects of vibration frequency on the parameters quantifying structural changes in the control and vibrated bone sections.
n=30 points from 6 rats for the control group, n=34 points from 9 rats for the 125 Hz group, n=40 points from 9 rats for the 250 Hz group. A) Empty lacunae count. B) Osteocyte count/total.

days of vibration groups, the number of empty lacunae are higher for 5D group as compared to control group (Fig. 2).

H&E stained bone sections were also evaluated for qualitative study of trabecular bone morphology of the control and vibrated bone (Fig. 3). The trabecular bone separation (Tb.Sp) appeared higher in the vibrated groups (Fig. 3C, 3H and 3I) as compared to the control group (Fig. 3A, 3D and 3G). The trabecular thickness (Tb.Th) appeared reduced in 1D group (Fig. 3B and 3C) compared to the 5D vibrated groups (Fig. 3D, 3E and 3F). Qualitatively, the Tb.Sp appears to be higher for the 20D time point (Fig. 3H and 3I) as compared to either 1D (Fig. 3A, 3B and 3C) or the 5D group (Fig. 3E and 3F).

Nitrotyrosine staining. Immunohistochemical staining was conducted on bone sections in order to assess the expression of NT protein, which is a marker of oxidative injury in the tissue. Figure 4 presents the qualitative changes observed due to NT immunostaining for all the groups. For the bone vibrated at 125 Hz and 250 Hz, brown color was also observed in bone marrow (BM). The cortical bone exhibited very little or no staining; hence, the NT stain values were not quantified. We observed that most of the positive signal was localized near the growth plate region of trabecular bone, which was in proximity to the bone marrow (BM). Qualitative observation shows that vibrated bone groups (125 Hz and 250 Hz) exhibited increased signal as compared to control bone. Similarly, the NT signal intensity in bone showed a higher intensity for all the time points of vibration (Fig. 4B, 4E and 4H, Fig. 4C, 4F and 4I).

Quantitative effects of vibration frequency on bone tissue alterations

Quantification of H&E Staining in Cortical Bone. In order to quantify the extent of structural alteration in the cortical bone, the number of osteocytes and empty lacunae were counted. The effects of vibration frequency on osteocyte and empty lacunae counts are summarized in Fig. 5. The number of empty lacunae in the bone tissue increased with increase in the vibration frequency (Fig. 5A). The empty lacunae count for the 250 Hz frequency group (10.82 ± 0.66) was statistically significant ($p<0.05$) in comparison to the control group (7.41 ± 0.76, Fig. 5A). For the 125 Hz

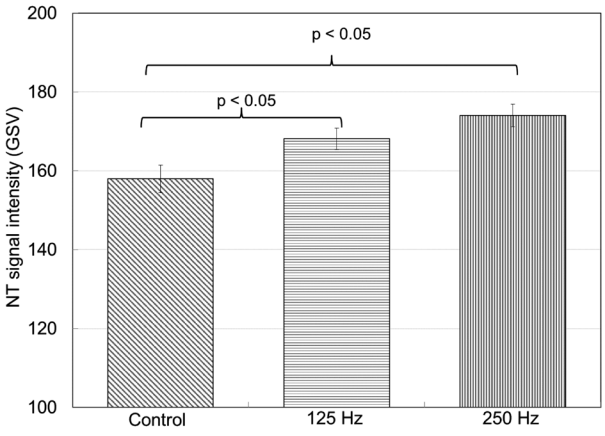

Fig. 6. Bar plot showing the effects of vibration frequency on the biological changes quantified using Nitrotyrosine signal intensity (GSV).
n=13 points from 6 rats for the control group, n=23 points from 9 rats for the 125 Hz group, n=19 points from 9 rats for the 250 Hz group.

group (9.09 ± 0.69), although an increase in the empty lacunae count was observed, the increase was insignificant (p=0.1) compared to the control group. The increase in empty lacunae count between 125 Hz and 250 Hz groups showed marginally significant p-value of 0.07.

Further, the ratio of the number of osteocytes to the total number of osteocytes and empty lacunae count (denoted as total) is quantified. An opposite trend was observed in this parameter, with the osteocyte count/total decreasing with an increase in the vibration frequency (Fig. 5B). The osteocyte count/total decrease was statistically significant for the 250 Hz frequency group (0.73 ± 0.01) as compared to control group (0.8 ± 0.02, Fig. 5B). The osteocyte count/total remained insignificant (p=0.13) for the 125 Hz group (0.76 ± 0.02) compared to control. Also, the decrease in count between 125 Hz and 250 Hz was insignificant (p=0.18). In summary, routine histology using H&E stain showed that 250 Hz causes highest number of empty lacunae with a corresponding reduced osteocyte count/total in the cortical bone.

Quantification of the Static Histomorphometry of Trabecular Bone. The extent of alterations in trabecular bone morphology was quantified using static histomorphometry. No significance was found for the effects of vibration frequency on Tb.Sp and Tb.Th considering p<0.05. The value of Tb.Sp for 125 Hz was 0.05 ± 0.005 mm, which remained almost the same (p=0.1) in comparison to the control group (0.04 ± 0.005 mm). The value of Tb.Sp for 250 Hz was 0.05 ± 0.004 mm, and showed no significance (p=0.2) compared to the control. Also, the value of Tb.Th

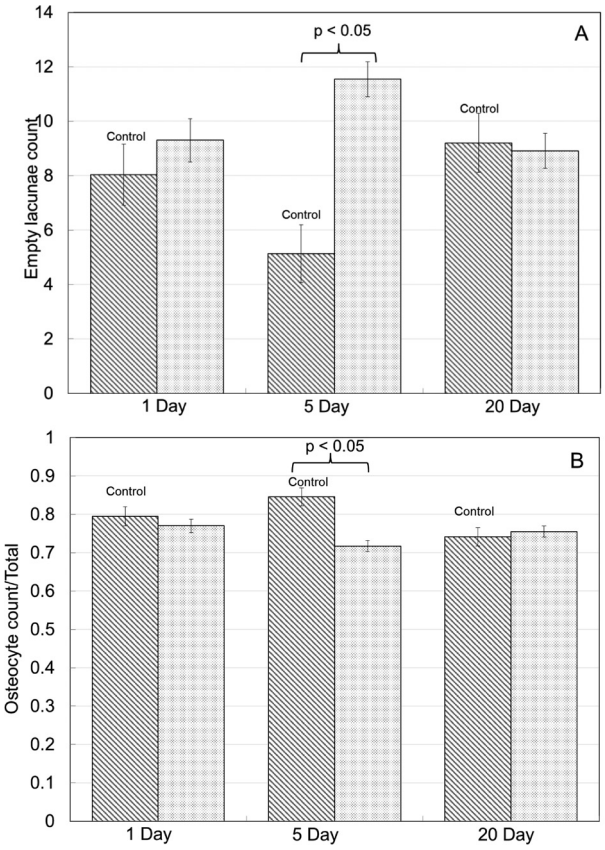

Fig. 7. Bar plots showing the effects of duration of vibration on parameters quantifying the structural changes in the bone tissue.
n=9 points from 2 rats for the control-1D group, n=11 points from 2 rats for the control-5D, n=10 points from 2 rats for the control-20D group. n=18 points from 6 rats for the 1D group, n=28 points from 6 rats for the 5D group, n=28 points from 6 rats for the 20D group. A) Empty lacunae count with individual control groups. B) Osteocyte count/total with individual control groups.

for the 125 Hz group was 0.10 ± 0.007 mm, and for the 250 Hz group was 0.09 ± 0.006 mm. Both the groups had insignificant changes compared to control group (0.10 ± 0.007 mm).

Overall, the trabecular bone morphology (represented by trabecular thickness and separation) was largely unaffected due to the frequency of vibration in comparison to the control group.

Quantification of the Nitrotyrosine Signal. The nitric oxide-dependent oxidative injury was quantified based on the NT signal intensity. The bar plots summarizing the effects of vibration frequency on NT signal intensity in the bone are shown in Fig. 6. As the vibration frequency increased, the NT signal intensity in the bone increased. In comparison to the control (157.99 ± 3.47 GSV), the NT Signal Intensity in trabecular bone was statistically sig-

nificant for both 125 Hz (168.12 ± 2.74 GSV) and 250 Hz (174.09 ± 2.89 GSV) frequency groups (Fig. 6).

In summary, these results demonstrate that structural disruption in cortical bone was significant at 250 Hz while the structural damage in the trabecular bone was insignificant at 125 Hz and 250 Hz. On the contrary, the biochemical changes, assessed by NT signal intensity, were significant at both 125 Hz and 250 Hz, for the trabecular bone.

Quantitative effects of vibration duration on bone tissue alterations

The effect of days of vibration exposure (1D, 5D, and 10D) on bone alterations were also assessed using the same methods discussed above. The H&E data and NT signal intensity data obtained from the control and different time points, 1D, 5D, and 20D (irrespective of the vibration group) were compared across the number of days of vibration.

Quantification in the Cortical Bone. The effects of days of vibration on the empty lacunae count (Fig. 7A) and Osteocyte count/total (Fig. 7B) are summarized in Fig. 7. Fig. 7A shows the bar plots comparing the empty lacunae counts in cortical bone for 1D, 5D and 20D vibration groups with their respective control groups. Empty lacunae count was statistically significant for 5D vibrated group (11.54 ± 0.64) compared to its own control group (5.13 ± 1.06). No statistical significance (p>0.05) was obtained for either the 1D vibrated group (9.3 ± 0.8) when compared to the 1D control group (8.03 ± 1.12) or the 20D vibrated group (8.91 ± 0.64) compared to the control group at 20D (9.2 ± 1.09). Vibration at 5D time point caused highest number of empty lacunae.

Figure 7B shows the bar plots comparing the osteocyte count/total in the cortical bone of the vibrated bone groups with their respective control groups, at different durations of vibration (1D, 5D and 20D). The osteocyte count/total was statistically significant for 5D vibrated group (0.72 ± 0.01) compared to the control group at 5D (0.85 ± 0.02). No statistical significance was obtained for either 1D vibrated group (0.77 ± 0.02) when compared to the 1D control group (0.79 ± 0.03) or the 20D (0.76 ± 0.01) compared to the control group at 20D (0.74 ± 0.02).

Overall, the results demonstrate that 5D time point caused highest number of empty lacunae with a corresponding reduced osteocyte count. Also, the reduction in empty lacunae count was significant between 5D and 20D time points.

Quantification in the Trabecular Bone. The Tb.Sp

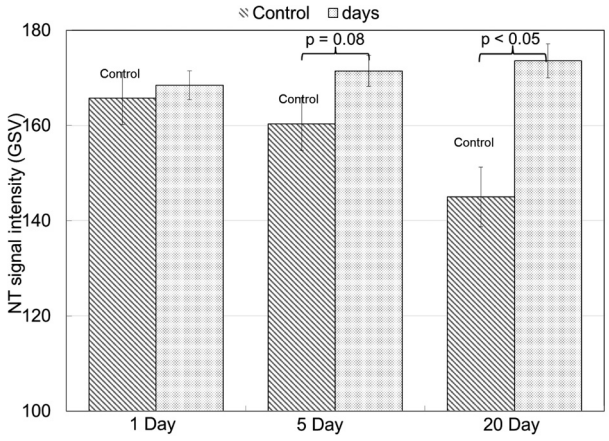

Fig. 8. Bar plots showing the effects of duration of vibration on biological changes quantified using Nitrotyrosine signal intensity (GSV).

n=5 points from 2 rats for the control-1D group, n=5 points from 2 rats for the control-5D, n=3 points from 2 rats for the control-20D group. n 18 points from 6 rats for the 1D group, n=14 points from 6 rats for the 5D group, n=10 points from 6 rats for the 20D group.

was statistically significant for the 20D group (0.06 ± 0.005 mm) as compared to control group (0.04 ± 0.004 mm). The increase in count between 5D (0.04 ± 0.004 mm) and 20D was also significant. No significance (p=0.05) was found for the 1D group (0.06 ± 0.005 mm) compared to control. Also, no significance was found (p=0.05) for the decrease in Tb.Sp between 1D and 5D groups. Similar results were obtained when comparisons were made between the vibrated groups and their respective control groups. Overall, these results show that trabecular spacing is dependent on the 20D time point of vibration and is lesser for vibrated group compared to control group.

The Tb.Th was not statistically significant for the 1D group (0.08 ± 0.008 mm) as compared to control group (0.10 ± 0.006 mm). Similarly, no significance (p=0.16) was found for the increase in count between 1D (0.04 ± 0.004 mm) and 5D group (0.10 ± 0.006 mm). Also, no significance was found (p=0.18) for the decrease in Tb.Th between 1D and 20D group (0.10 ± 0.005 mm). Similar results were obtained when comparisons were made between the vibrated groups and their respective control groups.

Overall, these results show that the trabecular spacing is dependent on vibration duration (20D) while trabecular thickness is not dependent on duration of vibration.

Quantification of the biochemical damage. Figure 8 shows the bar plot summarizing the effects of duration of

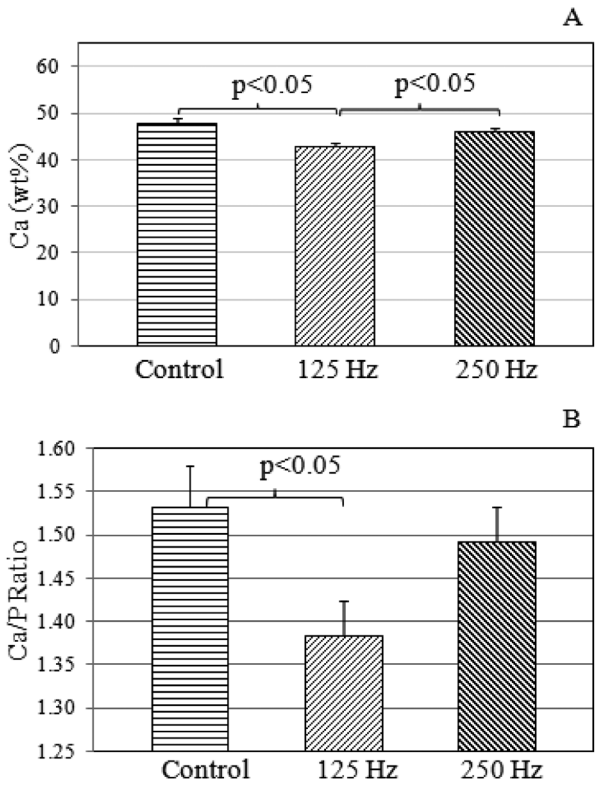

Fig. 9. Quantification of mineral content by EDX.
(A) Bar plot showing the effect of vibration frequency on Ca content (wt%); (B) Bar plot showing the effect of vibration frequency on Ca/P ratio of rat bone.

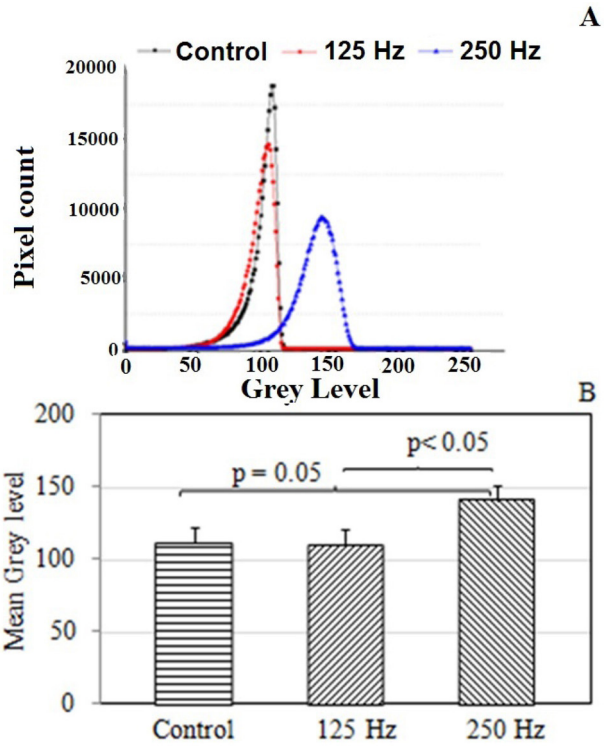

Fig. 10. Degree of Mineralization of bone from BSE images.
(A) shows the representative mineralization curve for bone for all the groups; (B) shows bar plot summarizing the degree of mineralization (denoted by mean grey level) for all the groups.

vibration on NT signal intensity in bone. A comparison of NT signal intensity at different time points with their respective control groups is provided. NT signal intensity in bone was statistically significant for 20D vibrated group (173.5 ± 3.5) compared to the control group at 20D (145.0 ± 6.3). The 5D vibrated group (171.4 ± 3.2) showed near significance *p*-value of 0.08, when compared to the control group at 5D (160.3 ± 5.4). No statistical significance at $p<0.05$ was obtained for the 1D vibrated group (168.4 ± 3.0) when compared to the 1D control group (165.7 ± 5.4).

Overall, these results show that biochemical damage increases with an increase in the duration of vibration exposure, with a significant effect observed at 20D time point.

Material testing on bone mineralization. In order to augment our histological methods, we performed material tests to assess the effect to vibration frequency on mineralization of the bone, at the 20D time point. The chemical composition of the bone was assessed using the%wt of Ca in the bone and the ratio of Ca/P. These results are summarized in the Fig. 9.

There was a significant decrease in the Ca at 125 Hz (42.99 ± 0.88) in comparison to the control group, while the 250 Hz (46.09 ± 0.85) remained insignificant compared to the control (47.79 ± 1.05). The increase in%wt of Ca was also significant between the 125 Hz and 250 Hz groups (Fig. 9A).

Similarly, the Ca/P ratio was significantly lower for 125 Hz (1.38 ± 0.04) compared to Control (1.53 ± 0.05, Fig. 9B), while no significance was found for 250 Hz (1.49 ± 0.04). However, the increase in Ca/P ratio from 125 Hz to 250 Hz was found to be marginally significant (p=0.07).

Further, assessment of the amount of mineralization in the bone tissue was performed. These results were summarized in Fig. 10. The mean grey level is an indicator of mineralization degree and a higher grey level signals higher mineralization (Fig. 10A). Quantification of these results show that 250 Hz causes higher degree of heterogeneous mineralization in bone and the mineralization is not as homogeneous as compared to either control or 125 Hz. 250 Hz showed significantly higher mineralization (141.18 ± 9.52) compared to control (111.3 ± 11.4). The increase in mineralization was also significant between 125 Hz (109.84 ± 11.43) and 250 Hz (Fig. 10B).

In summary, the Ca and Ca/P ratio were significant at 125 Hz while the bone mineralization was significant at 250 Hz. However, these results were assessed only at the 20D time point. In order to assess the duration effect, further studies are needed.

Discussion

We have studied vibration-induced bone tissue alterations in the form of structural damage, observed by: i) empty lacunae and osteocyte counts in cortical bone and changes in trabecular bone structure, and; ii) biochemical damage due to oxidative injury (NT formation). Results of this study show that the *structural damage was significant at 250 Hz for cortical bone* while it remained insignificant at both the frequencies for the trabecular bone. On the other hand, *the biochemical damage was significant at both the 125 Hz and 250 Hz* vibration frequencies.

Further, the results of this study show that the *structural damage was significant at 5D time point for the cortical bone* while the trabecular bone remained largely unaffected, with a change in trabecular spacing observed at 20D time point. The biochemical damage increased with increase in duration of vibration, *showing a significant change at 20D time point* and a near significant change at 5D time point.

A change in the NT signal intensity in the individual control groups at 1D, 5D, and 20D time point was observed. The NT signal intensity values decreased as the duration increased (Fig. 8B). However, this decrease was not statistically significant. Further, this decrease in NT signal intensity with an increase in the duration might be due to the acclimatization of the rats to the new environment and additionally due to the change in age of the rats. However, such changes need further investigation.

This study showed that bone alterations are dependent on duration of vibration. Present literature lacks comparison of NT staining on rat-tail bone tissue at *different time points of vibration*. Further, the biochemical response of trabecular bone and its oxidative damage due to the change in the duration of vibration remained unknown.

Effect of frequency of vibration. There are primarily three types of bone cells, namely osteoblasts, osteoclasts and osteocytes, that are expected to respond to vibratory stimulus. Osteocytes are the differentiated phenotype of osteoblasts and lie embedded in bone matrix, sensing loading through numerous sensory canalicular networks[35]. Study of these microscopic osteocytes under vibration can lead to improved assessment of the macroscopic dynamic characteristics of bone structure and any injury thereof.

In this study, an increased count of empty lacunae and decreased osteocyte count at 250 Hz was observed in the cortical bone. A previous study documented a reduced osteocyte density and higher number of empty lacunae in bones of osteoporotic sheep model[36]. Since osteocytes are the most abundant cells in bone matrix and are responsible for providing signals to osteoblasts (bone-forming cells), the decrease in their count along with increase in empty lacunae indicates that osteocytes are dying through either necrosis or apoptosis. Necrosis is more common in tissue damage due to external forces like heat, radiation, hypoxia or crushing of the tissue during handling. Apoptosis is a programmed phenomenon caused due to a stimulus leading to a specific pathway of cell death. Higher number of empty lacunae at 250 Hz indicate that this frequency may result osteocytes to undergo cell death, which might be due to a combination of both necrosis and apoptosis.

The balance between the osteocytes (bone-forming cells) and the osteoclasts (bone-resorption cells) is important to determine the bone structure. A previous study[37] has shown that low-magnitude vibrations in the frequency range of 20–90 Hz affect osteocytes, which in turn, respond by inhibiting the formation of osteoclasts. Another study[10] reported that at frequencies in the range of 5–100 Hz, in a dense bone, osteocyte cells oppose the presence of osteoclasts. Denser bone is more responsive to higher frequency (>100 Hz) loading. Hence, when denser bones are subjected to higher frequency vibrations (>100 Hz), the number of osteoclasts is lowered. These lower numbers of osteoclasts, in turn, stimulate the activity of osteoblasts. Hence, in denser bones, higher frequency vibrations (>100 Hz) might not degrade the bone tissue but might maintain it. On the other hand, less dense bones might suffer from degradation at higher frequency (>100 Hz) loading since the bone resorption is more pronounced due to the increased presence of osteoclast activity as opposed to the bone forming activity of osteoblasts. To explore this phenomenon in detail, further studies are warranted to explore cell death using stains specific to apoptosis, like cleaved caspase-3 stains or TUNEL assays.

Further, results of the present study on significant NT formation in bone are in agreement with previous studies. For example, a significant amount of NT staining was noted in femur metaphyses and chondrocytes in rats, after accumulation of iNOS protein[38]. Some researchers observed higher oxidative stress in the subchondral bone due to higher accumulation of NT[39]. To the best of our knowledge, this is probably the first study to report NT

formation in bone tissue under the influence of higher frequency of vibrations (125 Hz and 250 Hz), at various durations of vibration.

Effect of vibration on trabecular bone. The structure of bone displays spatial heterogeneity and is primarily composed of trabecular and cortical bone, which are structurally different and exhibit different rates of degeneration after a mechanical stimulus is applied[23]. In the literature, there are reports which document that trabecular bone is more sensitive to vibration loading[40]. An increased trabecular thickness and a reduced trabecular spacing have been documented in rat bones when a mechanical vibration stimulus was applied at a vibration frequency of 50 Hz[24]. Based on these studies, we assessed trabecular microarchitecture using two parameters: i) trabecular spacing (Tb.Sp); and ii) trabecular thickness (Tb.Th). Significant increase in Tb.Sp was observed for vibration at 20D time point; however, Tb.Th did not show significance at 20D. Perhaps, this increase in spacing might relate edematous changes, wherein excess fluid passes from the blood plasma to the tissue spaces through damaged endothelium. The discrepancy in the results of Tb.Th might be due to the higher frequency of vibrations, 125 Hz, and 250 Hz, used in this study as opposed to the lower frequencies (50 Hz) used in the previous studies[32, 33, 38]. Further studies are warranted to better evaluate the response of trabecular bone to different frequencies of vibrations.

Limitations. For this study, normal control group[41] has been used as opposed to rats sham-vibrated in restraints (restraint controls). The lack of restraint in a normal control group introduces additional bias. The rats in the normal control group have not been exposed to either constraint or vibration stress. Therefore, the use of restraint controls could be important to assess any additional variables introduced into the analysis. The authors acknowledge this as a limitation and consider it to be addressed in future study, when larger sample sizes are assessed.

The effect of frequency dependence that is near resonance range was investigated to evaluate vibration-induced bone tissue alterations by exposing rats to vibration of a constant acceleration of 49 m/s^2 RMS. These values were selected since the vibration frequency responses can be better assessed using rat-tail model[42] in workers who use hand held powered tools are frequently exposed to these vibration parameters (125 Hz, 250 Hz, 49 m/s^2). However, as reported in some studies, high impact vibrations, for example with frequencies <32.5 Hz might also lead to vibration injury. The effect of these frequencies needs to be explored in future studies.

The effect of variable vibration amplitude was not considered in the present study. Since HAVS is a complex disorder with interplay of vibration parameters of frequency, amplitude, acceleration and duration, future studies are warranted to give better assessment of vascular damage. In addition, the effect of energy constant condition as opposed to acceleration constant condition used in this study might somewhat affect the results. This effect would be explored in future studies. Further, gene expression studies to delineate the biochemical changes and mineralization studies to assess the material properties of bone using alkaline phosphatase marker are currently being considered. We also plan to investigate the role of sclerostin[43] produced by osteocytes under various vibration loading conditions. Lastly, the current study has a smaller sample size. Hence, the generalizability of the current findings is limited. The future plan is to augment the current results using a larger sample size.

Conclusions

In summary, structural alterations in the cortical bone occurred significantly at 250 Hz while biochemical alterations occurred significantly at both 125 Hz and 250 Hz. The trabecular bone remained unaffected due to change in vibration frequency. These findings demonstrate that bone damage is dependent on frequencies near resonance: 125 Hz and 250 Hz. Hence the current ISO guidelines might underestimate the bone damage at frequencies >100 Hz.

Also, the structural damage was significant at 5D for cortical bone while the trabecular bone showed significant damage at 20D time point. Further, the biochemical damage increased with increase in the duration of vibration with a significant damage observed at 20D time point and a near significant damage observed at 5D time point. Hence, the duration of vibration exposure might also play a role in elucidating degenerative changes in the bone tissue.

Acknowledgements

This work was supported by NIOSH-PRP grant: T42/OH008432-06. We would like to acknowledge the statistical guidance and advice provided by Dr. Paul Succop, Research Professor, Biostatistics, Department of Environmental Health, University of Cincinnati. The authors would like to thank Mr. Soumyarwit Manna for his considerable help with the material characterization analyses

of the bone tissue. The authors are grateful to Dr. Randall Allemang, Director of the Structural Dynamics Research Laboratory, for granting access to the vibration equipment.

References

1) Heaver C, Goonetilleke KS, Ferguson H, Shiralkar S (2011) Hand-arm vibration syndrome: a common occupational hazard in industrialized countries. J Hand Surg Eur Vol **36**, 354–63. [Medline] [CrossRef]
2) Bernard B, Nelson N, Estill CF Fine L, National institute of occupational safety and health (1998) The NIOSH review of hand-arm vibration syndrome: vigilance is crucial. J Occup Environ Med **40**, 780–5. [Medline] [CrossRef]
3) Griffin MJ (1990) Handbook of Human Vibration. Academic Press.
4) Gemne G, Saraste H (1987) Bone and joint pathology in workers using hand-held vibrating tools. An overview. Scand J Work Environ Health **13**, 290–300. [Medline] [CrossRef]
5) Javier-Moder RM, Kuntz JL (2003) Occupational bone diseases. Joint Bone Spine **70**, 414–21. [Medline] [CrossRef]
6) Jankovich JP (1972) The effects of mechanical vibration on bone development in the rat. J Biomech **5**, 241–50. [Medline] [CrossRef]
7) Min B (1998) Encyclopedia of occupational health and safety Vol. II (Ed. JM Stellman), 50.7–50.12, ILO, Geneva.
8) Griffin MJ, Bovenzi M (2002) The diagnosis of disorders caused by hand-transmitted vibration: Southampton Workshop 2000. Int Arch Occup Environ Health **75**, 1–5. [Medline]
9) Judex S, Rubin CT, RC JS (2010) Is bone formation induced by high-frequency mechanical signals modulated by muscle activity? J Musculoskelet Neuronal Interact **10**, 3–11. [Medline]
10) Bacabac RG, Smit TH, Van Loon JJWA, Doulabi BZ, Helder M, Klein-Nulend J (2006) Bone cell responses to high-frequency vibration stress: does the nucleus oscillate within the cytoplasm? FASEB J **20**, 858–64. [Medline] [CrossRef]
11) Dong RG, Schopper AW, McDowell TW, Welcome DE, Wu JZ, Smutz WP, Warren C, Rakheja S (2004) Vibration energy absorption (VEA) in human fingers-hand-arm system. Med Eng Phys **26**, 483–92. [Medline] [CrossRef]
12) Kihlberg S, Attebrant M, Gemne G, Kjellberg A (1995) Acute effects of vibration from a chipping hammer and a grinder on the hand-arm system. Occup Environ Med **52**, 731–7. [Medline] [CrossRef]
13) Krajnak K, Miller GR, Waugh S, Johnson C, Li S, Kashon ML (2010) Characterization of frequency-dependent responses of the vascular system to repetitive vibration. 584–94.
14) Govindaraju SR, Curry BD, Bain JLW, Riley DA (2008) Nerve damage occurs at a wide range of vibration frequencies. Int J Ind Ergon **38**, 687–92. [CrossRef]
15) Curry BD, Govindaraju SR, Bain JLW, Zhang LL, Yan JG, Matloub HS, Riley DA (2005) Evidence for frequency-dependent arterial damage in vibrated rat tails. Anat Rec A Discov Mol Cell Evol Biol **284**, 511–21. [Medline] [CrossRef]
16) Bovenzi M (1998) Exposure-response relationship in the hand-arm vibration syndrome: an overview of current epidemiology research. Int Arch Occup Environ Health **71**, 509–19. [Medline] [CrossRef]
17) Bovenzi M (2012) Epidemiological evidence for new frequency weightings of hand-transmitted vibration. Ind Health **50**, 377–87. [Medline] [CrossRef]
18) Chow JW, Jagger CJ, Chambers TJ (1996) Reduction in dynamic indices of cancellous bone formation in rat tail vertebrae after caudal neurectomy. Calcif Tissue Int **59**, 117–20. [Medline] [CrossRef]
19) Pazzaglia UE, Andrini L, Di Nucci A (1997) The effects of mechanical forces on bones and joints. Experimental study on the rat tail. J Bone Joint Surg Br **79**, 1024–30. [Medline] [CrossRef]
20) Guo XE, Eichler MJ, Takai E, Kim CH (2002) Quantification of a rat tail vertebra model for trabecular bone adaptation studies. J Biomech **35**, 363–8. [Medline] [CrossRef]
21) Tsukamoto N, Maeda T, Miura H, Jingushi S, Hosokawa A, Harimaya K, Higaki H, Kurata K, Iwamoto Y (2006) Repetitive tensile stress to rat caudal vertebrae inducing cartilage formation in the spinal ligaments: a possible role of mechanical stress in the development of ossification of the spinal ligaments. J Neurosurg Spine **5**, 234–42. [Medline] [CrossRef]
22) Kummari SR, Davis AJ, Vega LA, Ahn N, Cassinelli EH, Hernandez CJ (2009) Trabecular microfracture precedes cortical shell failure in the rat caudal vertebra under cyclic overloading. Calcif Tissue Int **85**, 127–33. [Medline] [CrossRef]
23) Al-Mufti RA, Williamson RCN, Mathie RT (1998) Increased nitric oxide activity in a rat model of acute pancreatitis. Gut **43**, 564–70. [Medline] [CrossRef]
24) Curtis CD, Thorngren DL, Nardulli AM (2010) Immunohistochemical analysis of oxidative stress and DNA repair proteins in normal mammary and breast cancer tissues. BMC Cancer **10**, 9. [Medline] [CrossRef]
25) Yan JGZL, Yan YH, Sanger JR, Jensen ES, Matloub HS (2010) Improved animal model for vibration injury study. scand. J. Lab. Anim. Sci. **37**, 159–69.
26) Qiu S, Rao DS, Palnitkar S, Parfitt AM (2002) Age and distance from the surface but not menopause reduce osteocyte density in human cancellous bone. Bone **31**, 313–8. [Medline] [CrossRef]
27) Doube M, Kłosowski MM, Arganda-Carreras I, Cordelières FP, Dougherty RP, Jackson JS, Schmid B, Hutchinson JR, Shefelbine SJ (2010) BoneJ: Free and extensible bone

image analysis in ImageJ. Bone **47**, 1076–9. [Medline] [CrossRef]
28) Goenka S, Peelukhana SV, Kim J, Stringer KF, Banerjee RK (2013) Dependence of vascular damage on higher frequency components in the rat-tail model. Ind Health **51**, 373–85. [Medline] [CrossRef]
29) Kingsmill VJ, Boyde A, Davis GR, Howell PG, Rawlinson SC (2010) Changes in bone mineral and matrix in response to a soft diet. J Dent Res **89**, 510–4. [Medline] [CrossRef]
30) Goldman HM, Bromage TG, Boyde A, Thomas CD, Clement JG (2003) Intrapopulation variability in mineralization density at the human femoral mid-shaft. J Anat **203**, 243–55. [Medline] [CrossRef]
31) Loveridge N, Power J, Reeve J, Boyde A (2004) Bone mineralization density and femoral neck fragility. Bone **35**, 929–41. [Medline] [CrossRef]
32) Gouin F, Passuti N, Verriele V, Delecrin J, Bainvel JV (1996) Histological features of large bone allografts. J Bone Joint Surg Br **78**, 38–41. [Medline]
33) Reddy Nagareddy P, Lakshmana M (2005) Assessment of experimental osteoporosis using CT-scanning, quantitative X-ray analysis and impact test in calcium deficient ovariectomized rats. J Pharmacol Toxicol Methods **52**, 350–5. [Medline] [CrossRef]
34) Diggle PJ, Heagerty P, Liang KY, Zeger SL (2002) Analysis of Longitudinal Data (2nd Ed.). Oxford Press.
35) Bonewald LF, Johnson ML (2008) Osteocytes, mechanosensing and Wnt signaling. Bone **42**, 606–15. [Medline] [CrossRef]
36) Zarrinkalam MR, Mulaibrahimovic A, Atkins GJ, Moore RJ (2012) Changes in osteocyte density correspond with changes in osteoblast and osteoclast activity in an osteoporotic sheep model. Osteoporos Int **23**, 1329–36. [Medline] [CrossRef]
37) Lau E, Al-Dujaili S, Guenther A, Liu D, Wang L, You L (2010) Effect of low-magnitude, high-frequency vibration on osteocytes in the regulation of osteoclasts. Bone **46**, 1508–15. [Medline] [CrossRef]
38) Cuzzocrea S, Mazzon E, Dugo L, Genovese T, Di Paola R, Ruggeri Z, Vegeto E, Caputi AP, Van De Loo FA, Puzzolo D, Maggi A (2003) Inducible nitric oxide synthase mediates bone loss in ovariectomized mice. Endocrinology **144**, 1098–107. [Medline] [CrossRef]
39) van der Harst M, Bull S, Brama PA, Barneveld AB, van Weeren PR, van de Lest C (2006) Nitrite and nitrotyrosine concentrations in articular cartilage, subchondral bone, and trabecular bone of normal juvenile, normal adult, and osteoarthritic adult equine metacarpophalangeal joints. J Rheumatol **33**, 1662–7. [Medline]
40) Ozcivici E, Luu YK, Rubin CT, Judex S (2010) Low-level vibrations retain bone marrow's osteogenic potential and augment recovery of trabecular bone during reambulation. PLoS ONE **5**, e11178. [Medline] [CrossRef]
41) Rowe DJ, Yan JG, Zhang LL, Pritchard KA Jr, Kao DS, Matloub HS, Riley DA (2011) The preventive effects of apolipoprotein mimetic D-4F from vibration injury-experiment in rats. Hand (NY) **6**, 64–70. [Medline] [CrossRef]
42) Welcome DE, Krajnak K, Kashon ML, Dong RG (2008) An investigation on the biodynamic foundation of a rat tail vibration model. Proc Inst Mech Eng H **222**, 1127–41. [Medline] [CrossRef]
43) Robling AG, Niziolek PJ, Baldridge LA, Condon KW, Allen MR, Alam I, Mantila SM, Gluhak-Heinrich J, Bellido TM, Harris SE, Turner CH (2008) Mechanical stimulation of bone in vivo reduces osteocyte expression of Sost/sclerostin. J Biol Chem **283**, 5866–75. [Medline] [CrossRef]

Appendix 1.

Interaction effects on structural and biochemical damage

A summary of the 1-way ANOVA analyses between the groups, Control-1D, 125 Hz-1D, 250 Hz-1D; Control-5D, 125 Hz-5D, 250 Hz-5D; Control-20D, 125 Hz-20D, and 250 Hz-20D, is presented in Fig. 11. The interaction effects of groups of vibration frequency and days of vibration on structural parameters, empty lacunae count and Osteocyte count/total is presented in Fig. 11A, and Fig. 11B, respectively. The interaction effects of groups on biochemical parameter, NT signal intensity is presented in Fig. 11C.

The empty lacunae count was not statistically significant ($p>0.05$; Fig. 11A) for 125 Hz-1D group (8.4 ± 1.1) and 250 Hz-1D group (10.1 ± 0.9) compared to the control group at 1D (8.0 ± 0.9). On the other hand, the 125 Hz-5D group (10.8 ± 0.9) and the 250 Hz-5D group (12.2 ± 0.8) showed significant ($p<0.05$) difference in comparison to the 5D control group (5.1 ± 0.9). No statistical significance ($p>0.05$) was obtained for either 125 Hz-20D group (7.8 ± 0.9) or the 250 Hz-20D group (9.9 ± 0.8) when compared to the 20D control group (9.2 ± 0.9).

The osteocyte count/total was not statistically significant ($p>0.05$; Fig. 11B) for 125 Hz-1D group (0.78 ± 0.03) and 250 Hz-1D group (0.76 ± 0.02) compared to the control group at 1D (0.79 ± 0.02). On the other hand, the 125 Hz-5D group (0.73 ± 0.02) and the 250 Hz-5D group (0.74 ± 0.02) showed significant difference ($p<0.05$) in comparison to the 5D control group (0.85 ± 0.02). No statistical significance ($p>0.05$) was obtained for either 125 Hz-20D group (0.78 ± 0.02) or the 250 Hz-20D group (0.74 ± 0.02) when compared to the 20D control group (0.74 ± 0.02).

The NT signal intensity was not statistically significant ($p>0.05$; Fig. 11C) for 125 Hz-1D group (167.6 ± 3.6) and 250 Hz-1D group (169.3 ± 3.9) compared to the control group at 1D (165.7 ± 4.8). On the other hand, the 125 Hz-5D group (171.8 ± 4.0) was statistical ($p<0.05$) significance in comparison to the 5D control group (160.4 ± 3.9) while the 250 Hz-5D group (170.9 ± 4.1) showed borderline significant ($p=0.08$) difference in comparison to the 5D control group (160.4 ± 3.9). Further, statistical significance ($p<0.05$) was obtained for both the 125 Hz-20D group (164.4 ± 4.3) and the 250 Hz-20D group (184.8 ± 4.8) when compared to the 20D control group (144.9 ± 5.7).

Overall, these results show a significant change in the structural parameters at both the 125 Hz and 250 Hz at the 5D timepoint. Similarly, the biochemical damage was significant at 125 Hz vibration at 5D and borderline significant at 250 Hz-5D. The biochemical damage was significant at the 20D time point for both the 125 Hz and 250 Hz.

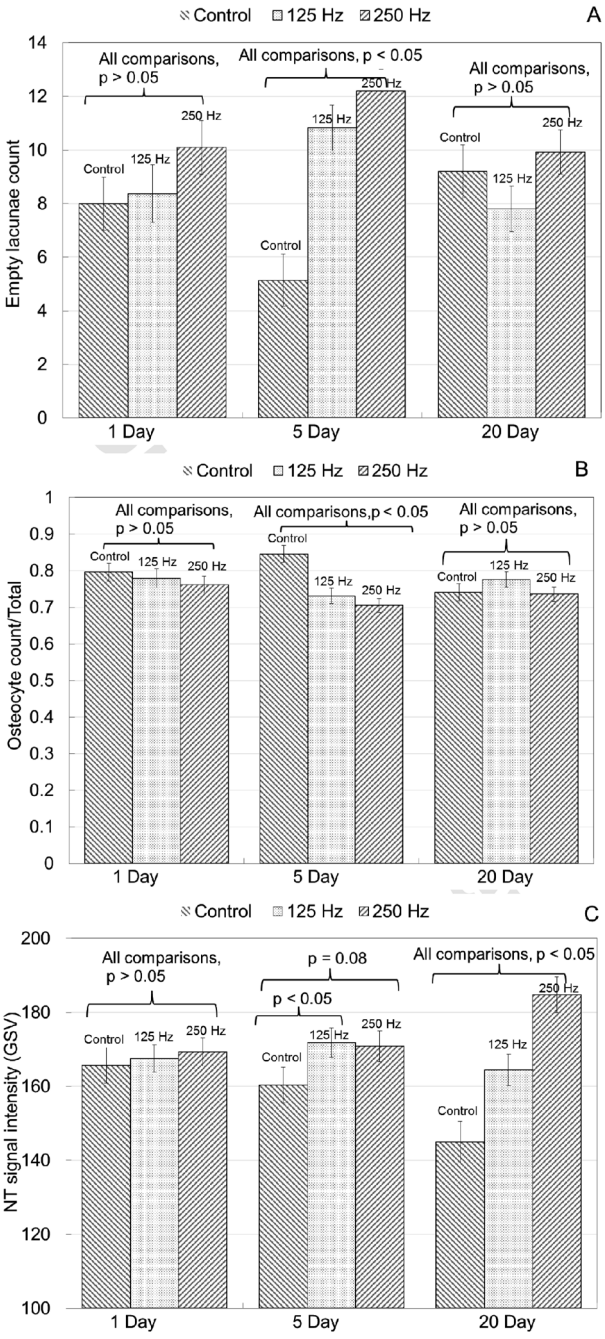

Fig. 11. Bar plots showing the effects of vibration frequency and duration on the structural and biological changes occurring in the interaction groups.

A) Empty lacunae count. n=9 points from 2 rats for the control-1D group, n=11 points from 2 rats for the control-5D, n=10 points from 2 rats for the control-20D group. N=8 points from 3 rats for the 125 Hz-1D group, n=13 points from 3 rats for the 125 Hz-5D group, n=13 points from 3 rats for the 125 Hz-20D group. N=10 points from 3 rats for the 250 Hz-1D group, n=15 points from 3 rats for the 250 Hz-5D group, n=15 points from 3 rats for the 250 Hz-20D group. B) Osteocyte count/total. The sample size is the same as the above. C) Nitrotyrosine signal intensity (GSV). N=5 points from 2 rats for the control-1D group, n=5 points from 2 rats for the control-5D, n=3 points from 2 rats for the control-20D group. N=10 points from 3 rats for the 125 Hz-1D group, n=7 points from 3 rats for the 125 Hz-5D group, n=6 points from 3 rats for the 125 Hz-20D group. N=8 points from 3 rats for the 250 Hz-1D group, n=7 points from 3 rats for the 250 Hz-5D group, n=4 points from 3 rats for the 250 Hz-20D group.